scientific reports

Check for updates

OPEN

Vibrio natriegens as a superior host for the production of c-type cytochromes and difficult-to-express redox proteins

Helena Fuchs✉, Sophie R. Ullrich & Sabrina Hedrich✉

C-type cytochromes fulfil many essential roles in both aerobic and anaerobic respiration. Their characterization requires large quantities of protein which can be obtained through heterologous production. Heterologous production of c-type cytochromes in *Escherichia coli* is hindered since the *ccmABCDEFGH* genes necessary for incorporation of heme c are only expressed under anaerobic conditions. Different strategies were devised to bypass this obstacle, such as co-expressing the *ccm* genes from the pEC86 vector. However, co-expression methods restrict the choice of expression host and vector. Here we describe the first use of *Vibrio natriegens* V_{max} X2 for the recombinant production of difficult-to-express redox proteins from the extreme acidophile *Acidithiobacillus ferrooxidans* CCM4253, including three c-type cytochromes. Co-expression of the *ccm* genes was not required to produce holo-c-type cytochromes in V_{max} X2. *E. coli* T7 Express only produced holo-c-type cytochromes during co-expression of the *ccm* genes and was not able to produce the inner membrane cytochrome CycA. Additionally, V_{max} X2 cell extracts contained higher portions of recombinant holo-proteins than T7 Express cell extracts. All redox proteins were translocated to the intended cell compartment in both hosts. In conclusion, *V. natriegens* represents a promising alternative for the production of c-type cytochromes and difficult-to-express redox proteins.

Cytochromes play essential roles as electron carriers during both aerobic and anaerobic respiration in all organisms. They all contain heme as a co-factor. The heme c co-factor in c-type cytochromes (Cytc) is covalently bound to the protein. The consensus motif, CXXCH, of Cytc contains two highly conserved cysteine residues which form thioether bonds with the heme while the histidine acts as an axial ligand to the iron[1].

The ability to produce large quantities of protein during heterologous expression is essential for the characterization and study of novel as well as known proteins. C-type cytochromes pose one of the greatest challenges for heterologous production due to the extensive post-translational modifications required to produce holo-Cytc (Fig. 1). While gene transcription and translation take place in the cytoplasm, c-type cytochromes are known to function as soluble periplasmic proteins (or soluble proteins in the intermembrane space of mitochondria) or membrane-anchored proteins[2]. Therefore, the apo-protein needs to be translocated across the inner membrane into the periplasm. Heme synthesis also has a resource demand on host cells, especially during over-expression. After heme is transported into the periplasmic space, a set of eight proteins is required to deliver the heme to the apo-Cytc and facilitate covalent attachment in *Escherichia coli*. These proteins are termed CcmABCDEFGH for cytochrome c maturation and are located on the periplasmic site of the inner membrane[3–5]. *E. coli* expression strains, such as BL21(DE3) and T7 Express, possess chromosomal copies of the corresponding genes. They are part of the *aeg46.5* operon which is not active under aerobic conditions[6]. As a consequence, the production of holo-Cytc is not possible in aerobically grown *E. coli* cells. To circumvent this, a strategy for the co-expression of the *ccmA-H* genes from an additional plasmid, termed pEC86, was developed. This enables the production of holo-Cytc under aerobic conditions[2,7]. Additionally, heme pre-cursors, such as δ-aminolevulinic acid (δ-ALA), can be supplemented to overcome bottlenecks in heme biosynthesis[8]. Heme can also be directly supplemented to the culture medium when heme uptake systems are co-expressed in *E. coli*[9,10]. However, these co-expression

TU Bergakademie Freiberg, Institute of Biosciences, Leipziger Straße 29, 09599 Freiberg, Germany. ✉email: helena.fuchs@student.tu-freiberg.de; sabrina.hedrich@bio.tu-freiberg.de

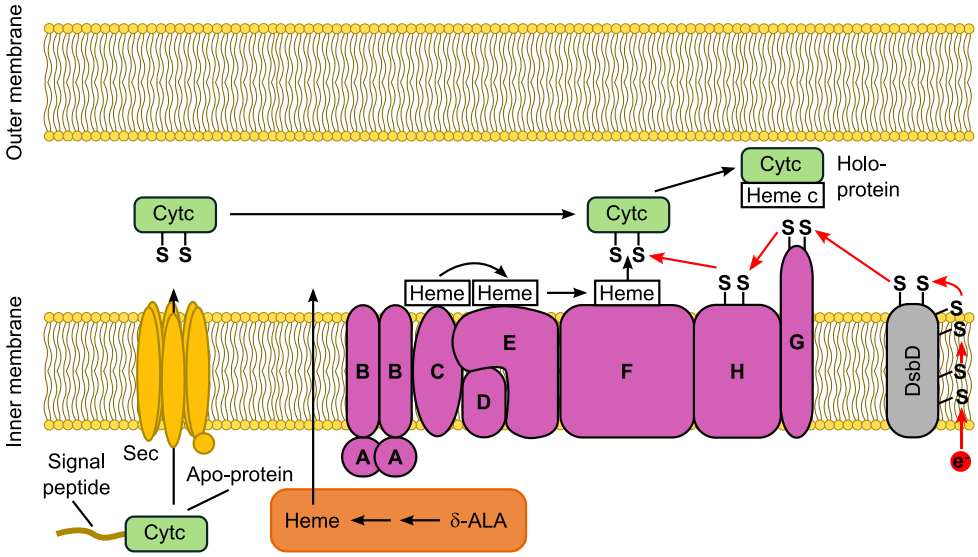

Figure 1. Post-translational modifications required for the production of holo-c-type cytochromes (Cytc) in *E. coli*[3–5]. Transcription and translation of the Cytc encoding gene and mRNA take place in the cytoplasm while co-factor integration and folding occur in the periplasm. The signal peptide of the apo-protein leads to translocation into the periplasm via the general secretory (Sec) translocation pathway[29]. Heme is synthesized in the cytoplasm from δ-aminolevulinic acid (δ-ALA), transported into the periplasm and delivered to the apo-Cytc via CcmC, CcmE, and CcmF. CcmF catalyzes the covalent attachment of heme to the cysteine residues of the Cytc binding motif. CcmA and CcmB are predicted to be transporter proteins. However, it is unclear what substrate they transport. CcmD stabilizes CcmE in the membrane. Electrons required for the formation of the thioether bonds are delivered to the apo-Cytc via CcmH, CcmG, and DsbD. After integration of heme c and folding, holo-Cytc remains soluble in the periplasm or is integrated into a membrane.

methods restrict the choice of expression host, vector, selection marker, and can also negatively impact growth and yield.

Here, we describe a different expression host, the marine bacterium *Vibrio natriegens*, for the production of difficult-to-express redox proteins, including three c-type cytochromes from the extreme acidophile *Acidithiobacillus ferrooxidans* CCM4253. *V. natriegens* (initially referred to as *Pseudomonas natriegens*) is an emerging host for heterologous protein production with a remarkable doubling time of under ten minutes[11], making it the fastest growing bacterium known to date. It's greater biomass synthesis rate and stronger protein expression ability[12] are partially caused by the 20–40% higher ribosome number per cell compared to *E. coli*[13]. *V. natriegens* grows well on various industrially relevant substrates and exhibits a higher feedstock flexibility compared to *E. coli*[14,15]. Additionally, there is already a wide array of genetic tools available for *V. natriegens,* such as expression vectors with various backbones, promoters, and tags[16–18]. Protocols for DNA transformation based on electroporation and heat shock[16,19], methods to manipulate gene expression via CRISPR interference (CRISPRi)[20], as well as genome editing techniques based on multiplex genome editing by natural transformation (MuGENT)[21] and natural transformation CRISPR (NT-CRISPR)[22] have also been established. The strain V_{max} X2 was engineered from the type strain ATCC 14048 by inserting a T7 RNA polymerase cassette under the control of a *lacUV5* promotor in the *dns* locus[16]. *V. natriegens* has been shown to produce soluble periplasmic[17] as well as the functional multi-subunit membrane protein complex NADH:quinone oxidoreducase (NQR) and the secondary transport system Mrp from *Vibrio cholerae*[23]. Eichmann et al.[17] showed that production of the difficult-to-express proteins lucimycin and uricase was higher in *V. natriegens* than *E. coli* BL21(DE3) and Becker et al.[24] demonstrated higher production levels for isotopically labelled FK506 binding protein (FKBP) as well as enhanced yellow fluorescent protein (EYFP) in *V. natriegens* compared to *E. coli* BL21(DE3). Xu et al.[25] also demonstrated that *V. natriegens* has a complementary expression spectrum to *E. coli*. Proteins that *E. coli* failed to produce in a soluble state were produced as soluble proteins in *V. natriegens* with up to 12 times higher expression. In addition, *V. natriegens* seems to have an extremely broad over-expression spectrum encompassing more than six enzyme families from bacterial, fungal, and plant origin. *V. natriegens* also produced higher amounts of an archaeal catalase-peroxidase (AfKatG) compared to *E. coli* BL21(DE3)[26]. A particular advantage is the production of smaller soluble proteins, which might be helpful in avoiding bottlenecks (i.e. translocation and folding) during the production of soluble periplasmic proteins with *E. coli*[25].

In this study, we compared the production of three c-type cytochromes, the inner membrane-anchored CycA, the soluble periplasmic Cytc Cyc1, and the outer-membrane Cytc Cyc2, as well as the soluble blue copper protein rusticyanin (Rus) in *V. natriegens* V_{max} X2 and *E. coli* T7 Express. V_{max} X2 proved to be a promising expression host for the production of difficult-to-express Cytc. In contrast to T7 Express, V_{max} X2 did not require co-expression of the *ccm* genes from a second plasmid to produce holo-Cytc.

Results and discussion

Genes encoding the c-type cytochromes CycA, Cyc1, and Cyc2 were co-expressed with the Rus encoding gene from *At. ferrooxidans* CCM4253 in order to compare the performance of V_{max} X2 and T7 Express regarding their ability to produce recombinant redox proteins. All gene sequences were codon optimized for *E. coli* K-12. Gene and protein sequences are listed in Supplementary Note 1. The strains and plasmids used in this study are listed in Supplementary Table 1. All proteins are part of the electron transfer chain of *At. ferrooxidans* for the reduction of ferric iron under anaerobic conditions[27]. CycA is anchored to the inner membrane on the periplasmic site, while Cyc1 and Rus are soluble periplasmic proteins. Cyc2 is a typical β-barrel protein[28] that is fully integrated into the outer membrane. N-terminal signal peptides for translocation across the inner membrane via the general secretory (Sec) pathway[29] were predicted for all proteins. Gene sequences used for the heterologous expression contained the unmodified native signal peptide sequences.

V. natriegens produces higher amounts of holo-rusticyanin

Vibrio natriegens V_{max} X2 and *E. coli* T7 Express containing either both the pEC86 and pET16bP_cycA_cyc1_rus_cyc2 vectors or only the pET16bP_cycA_cyc1_rus_cyc2 vector (Supplementary Table 1) were used to heterologously produce rusticyanin from *At. ferrooxidans* CCM4253. The periplasm, cytoplasm, and membranes were separated to determine correct translocation. Rus was detected via immunodetection with specific antibodies after separation by SDS-PAGE and subsequent western blotting. Apo-Rus with the attached signal peptide has a size of 19.9 kDa, while holo-Rus, from which the signal peptide was cleaved, was detected at the expected weight (16.6 kDa) (Fig. 2a).

While both strains were able to produce holo-Rus, it seems to comprise a greater relative portion of the total protein in V_{max} X2 cell extracts. The natural signal peptide was recognized and cleaved in both strains, evident from the holo-Rus detected in their periplasm. Apart from the periplasm, holo-Rus was also detected in all other

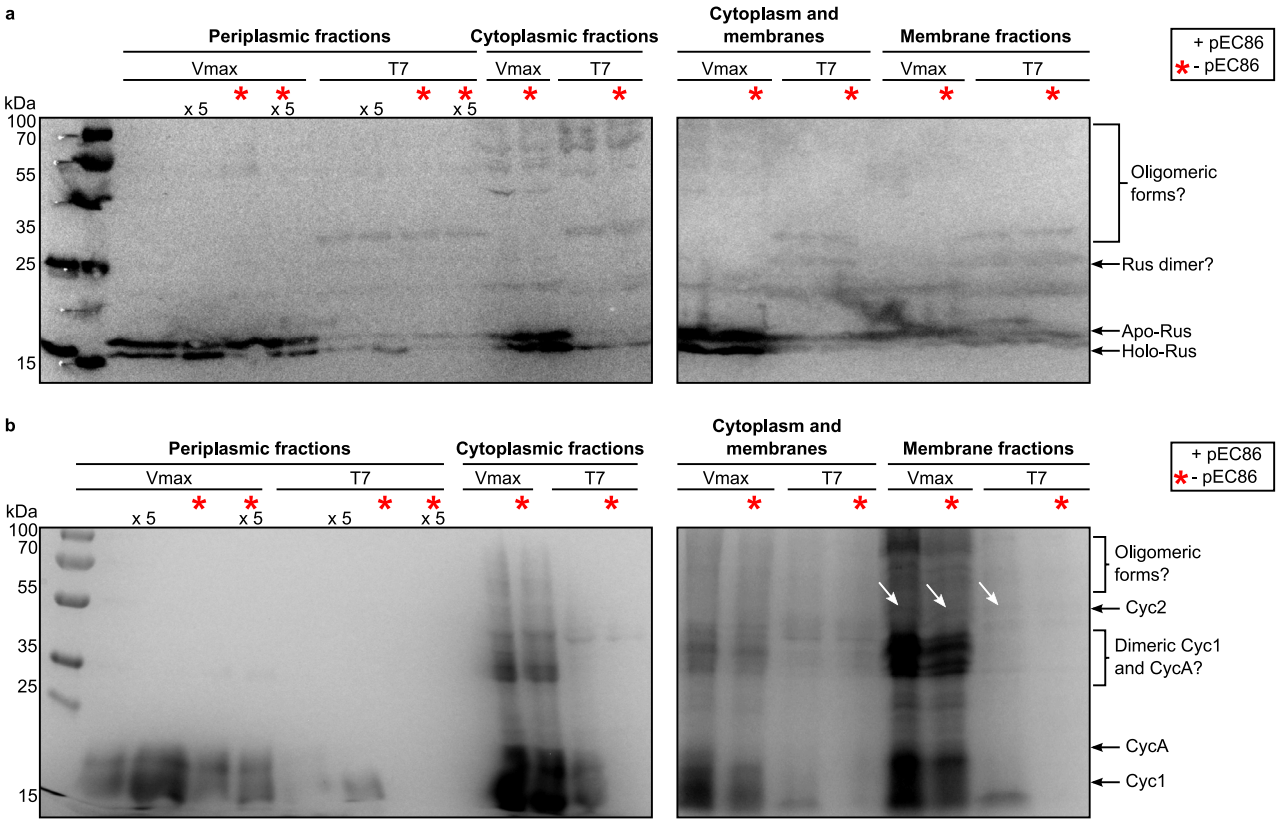

Figure 2. Immunodetection of rusticyanin (Rus) and 3,3′,5,5′-tetramethylbenzidine (TMBZ) stain for the detection of holo-c-type cytochromes. Fresh cells were fractionated according to Petiti et al.[50]. Protein concentrations of each fraction were determined with a BCA assay in triplicates. For unconcentrated fractions, 150 µg total protein was loaded onto SDS-PAGE gels, 300 µg total protein was loaded for the concentrated periplasmic fractions (x 5). All samples, gels, Western blots, and immunodetections were processed in parallel. Samples from cells without the pEC86 plasmid are marked with a red star. (**a**) Immunodetection of Rus in protein extracts from different cell compartments. A holo-Rus positive control (0.33 µg), isolated from *At. ferrooxidans*, was loaded left to the molecular weight marker. Holo-Rus possesses a molecular weight of 16.6 kDa and apo-Rus 19.9 kDa. (**b**) TMBZ-stain[34] of holo-c-type cytochromes in protein extracts from different cell compartments. The cytochromes possess the following molecular weights: (1) holo-Cyc1 20.0 kDa, (2) holo-CycA 22.3 kDa, (3) holo-Cyc2 49.3 kDa. The bands corresponding to Cyc2 are marked with white arrows.

cell compartments. Since the signal peptide is cleaved during translocation into the periplasm, holo-Rus should not be present in the cytoplasm. However, Rus tends to associate itself with the membranes of the neutrophilic hosts and can be resolubilized by washing with an acidic buffer (Supplementary Fig. 1). Therefore, membrane association likely occurs via weak electrostatic interactions due to a different surface charge at neutral pH. This corresponds to the very high predicted pI of 8.0 for holo-Rus (Supplementary Note 2). Bengrine et al.[30] also described weak attachment of Rus to the cell membranes of *E. coli* expression hosts combined with a lack of soluble Rus in the periplasmic fraction. Native Rus was also associated to the membranes of *At. ferrooxidans* in different studies[31,32] rather than remaining soluble in the periplasm when cells were lysed by sonication and French press at pH 7 instead of pH 2. This corroborates our assumption that membrane association is caused by a different surface charge at neutral pH. Fully matured periplasmic proteins could have also been detected in the cytoplasmic fraction because some cells remained intact during the osmotic shock. This is especially relevant for V_{max} X2 since Rus seems to comprise a greater relative portion of the total protein in the samples. In order to minimize the portion of intact cells, dissociation of the outer membrane was monitored microscopically by observing cell morphology and movement. Membrane-associated Rus also may have been detached from the membranes and solubilized during sonication of the spheroplasts with some remaining associated to the membranes.

Rus from *At. ferrooxidans* seems to occur as a monomer and dimer, judging from the size of the higher molecular weight band. Rus is predicted to function as a monomer and may form a respiratory super-complex with Cyc1 and Cyc2[28,33]. Therefore, it is unclear whether the dimer also fulfils a role in electron transfer or if it is just a result of sample preparation before SDS-PAGE. Oligomeric forms were also detected in the neutrophilic hosts V_{max} X2 and T7 Express, with T7 Express forming more oligomers, especially supposed dimers of the apo- and holo-protein.

Holo-c-type cytochromes are produced in *V. natriegens* without co-expression of the *ccm* genes

The periplasm, cytoplasm, and membranes were separated to determine correct translocation. Holo-Cytc was detected via TMBZ-staining[34] after separation by SDS-PAGE. Since SDS-PAGE was performed under denaturing conditions, only covalently bound hemes, i.e. heme c, were detected. Holo-Cyc1 had a size of 20.0 kDa, Holo-CycA possessed a molecular weight of 22.3 kDa, and Holo-Cyc2 had a size of 49.3 kDa (Fig. 2b).

V_{max} X2 produced all holo-c-type cytochromes under all conditions, while holo-CycA was not detected in T7 Express. Additionally, T7 Express was not able to produce any of the tested Holo-Cytc when the *ccmA-H* genes were not co-expressed (marked with red star in Fig. 2). The soluble periplasmic Cytc, Cyc1, was also detected in other compartments besides the periplasm, similar to Rus. Since an even higher pI of 8.86 was predicted for holo-Cyc1 (Supplementary Note 2), the protein was likely also weakly associated to the membranes and was washed off the membranes with an acidic buffer (Supplementary Fig. 1). The other two membrane-anchored or bound cytochromes were only detected in the membrane fractions. The band intensity of Holo-Cyc2 (marked with white arrows in Fig. 2b) after heme-staining is very low since it harbours only one heme c binding site[28] while CycA and Cyc1 are diheme cytochromes. As with Rus, oligomeric forms of the cytochromes were also detected in the TMBZ-stained extracts of V_{max} X2 and T7 Express, with the most prominent bands presumably representing dimeric forms of Cyc1 and CycA just above the 35 kDa marker band (Fig. 2b). High-molecular weight aggregates of the cytochromes were also detected. The band intensities in Fig. 2b suggest a greater relative portion of holo-Cytc in V_{max} X2 cell extracts, which is supported by UV/Vis spectra recorded from the soluble fractions (Fig. 3).

Cell extracts and membrane pellets obtained from V_{max} X2 during fractionation appeared reddish, indicating the presence of holo-Cytc (Fig. 3a). UV/Vis spectra of Na-dithionite treated fractions from V_{max} X2 (Fig. 3b–d) revealed higher absorbance intensities, corresponding to a higher Cytc content. The absorbance maxima of the α- and β-peak of T7 Express without the pEC86 plasmid are different than those of the other extracts (Fig. 3d). Typically, heme c exhibits absorbance maxima at 410 nm (γ-peak), 525 nm (β-peak), and 550 nm (α-peak) in its reduced state. These maxima are shifted to slightly longer wavelengths in heme b[1,2,35]. Such heme b specific peaks were detected in fractions of T7 Express without the pEC86 vector, suggesting that only host-derived b-type cytochromes were enriched. This can be attributed to the heme b co-factor of the cytochrome bo_3[36] and cytochrome *bd-I*[37,38] ubiquinol oxidases of *E. coli*, demonstrating that T7 Express produced no detectable amount of heme c under aerobic conditions, as described previously[2,7]. Absorbance maxima corresponding to heme c were only detected when the *ccm* genes were co-expressed. However, expression levels in T7 Express were very low. In contrast, heme c was also detected in extracts from aerobically grown V_{max} X2 cells which did not carry the pEC86 plasmid. Peak shoulders corresponding to heme b were also detected in V_{max} X2 protein extracts. This strain most likely also natively produces b-type cytochromes since genes predicted to encode subunits of a cytochrome *bd-I* (*cydABX*) and cytochrome bo_3 (*cyoA-D*) oxidase are located on chromosome 1 and 2 of *V. natriegens* ATCC 14048 respectively.

The difference in expression levels of holo-Cytc in V_{max} X2 cells carrying the pEC86 plasmid to cells without the pEC86 plasmid seems to be negligible, while the presence of the pEC86 vector in T7 Express cells only leads to low expression levels of holo-Cytc. This makes *V. natriegens* an interesting production host for recombinant c-type cytochromes.

The spectra in Fig. 3c demonstrate that recombinant Cytc produced by V_{max} X2 and T7 Express was redox-active. Upon sample preparation, heme c was completely reduced and could be oxidized by adding up to 10 mM $Na_2[IrCl_6]$. The α- and β-peaks disappeared upon oxidation and were replaced by a broad plateau. Additionally, the γ-peak shifted to slightly shorter wavelengths[1,2,35]. Oxidized heme c was re-reduced upon addition of sodium dithionite (Supplementary Fig. 2). This redox activity suggests that heme c was integrated in the heterologous c-type cytochromes despite the difference in extracellular and periplasmic pH. Considering that holo-CycA was

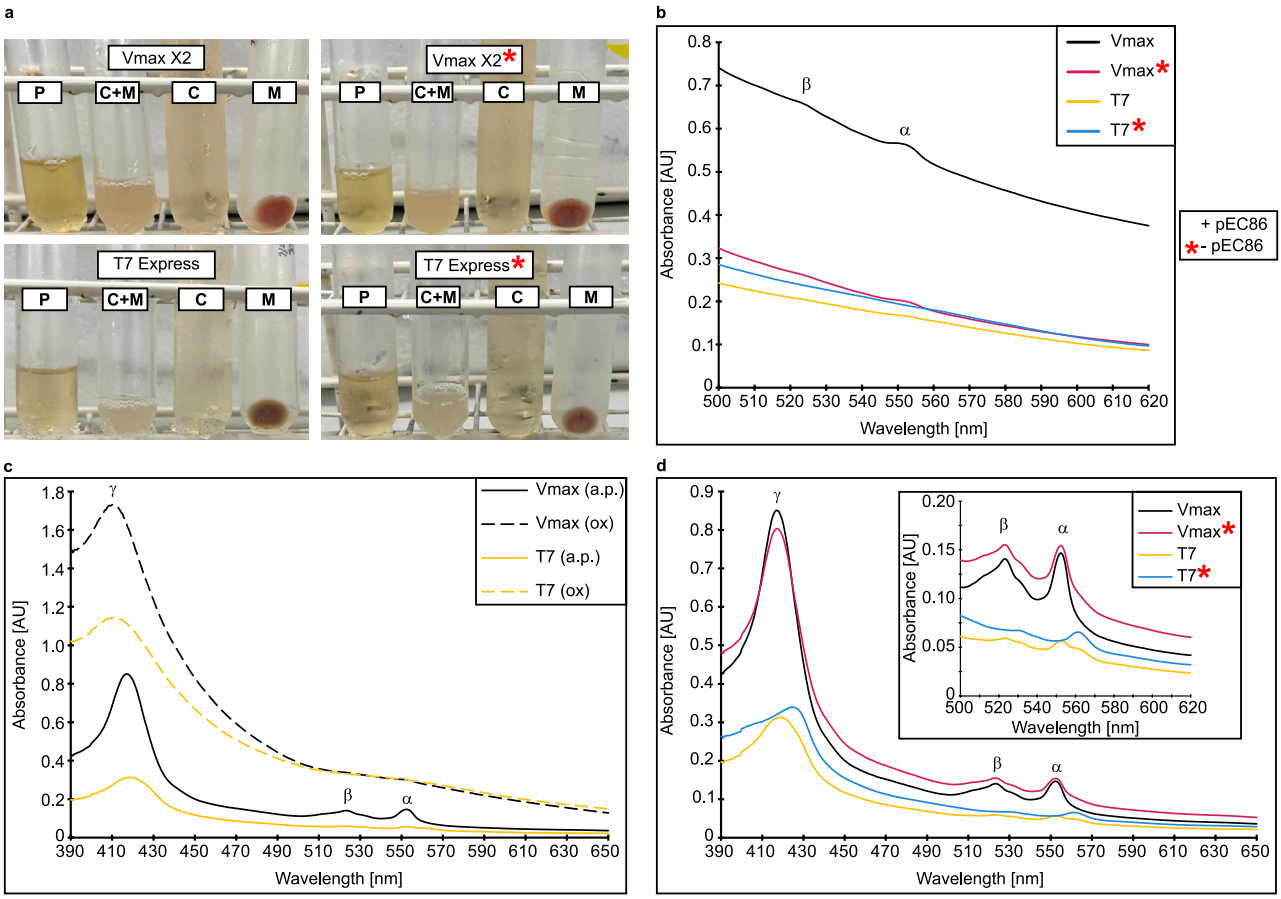

Figure 3. UV/Vis spectra of protein extracts from different cell compartments of V_{max} X2 and T7 Express. Fresh cells were fractionated according to Petiti et al.[50]. A 100 µL sample was used for each measurement. Measurements were performed in TES buffer diluted 1:2 in water at pH 8.0. The periplasmic fractions were concentrated five times in centricons with a molecular weight cut-off of 10 kDa. Strains without the pEC86 plasmid are labelled with a red star. V_{max} X2 carrying the pEC86 plasmid is coloured in black, V_{max} X2 without pEC86 in red, T7 Express with pEC86 in yellow, and T7 Express without pEC86 in blue. Spectra of reduced samples are displayed with solid lines and spectra of oxidized samples with dashed lines. The three characteristic absorbance maxima of reduced heme c are labelled α (550 nm), β (525 nm), and γ (410–420 nm) respectively[1,2,35]. Oxidation was achieved by the addition of up to 10 mM $Na_2[IrCl_6]$, and reduction by adding Na-dithionite. (**a**) Pictures of cell compartment fractions after preparation. Legend: P—periplasmic fraction; C + M—cytoplasm and membranes; C—cytoplasmic fraction; M—membrane fraction. (**b**) Comparison of the α- and β-peaks of heme in the periplasmic fractions. (**c**) Comparison of spectra of reduced (a.p.) and oxidized (ox) heme c in the cytoplasm of V_{max} X2 and T7 Express with pEC86. (**d**) Comparison of UV/Vis spectra of the cytoplasmic fractions of V_{max} X2 and T7 Express with and without pEC86. The absorbance maxima in the cytoplasmic fraction of T7 Express without pEC86 are shifted to slightly longer wavelengths, indicating the presence of heme b instead of heme c[1,2,35].

not detected in *E. coli* protein extracts (Fig. 2b), *V. natriegens* seems to be a more suitable host for the production of difficult-to-express redox proteins from extreme acidophiles.

Additionally, *V. natriegens* V_{max} X2 exhibited faster growth than *E. coli* T7 Express, especially in the early exponential growth phase (Supplementary Fig. 3), resulting in a time saving of several hours during experiments. Fast growth of *V. natriegens* was observed by us in traditional *E. coli* media (e.g. LB, 2xYT, e2xYT) at temperatures of 20–37 °C, while the fastest growth was achieved by supplementing 15 g L^{-1} NaCl[14] or a mixture of NaCl, KCl, and $MgCl_2$[16] at 30 °C and 37 °C. *V. natriegens* also produced 35% more biomass (cell wet weight, Supplementary Table 4) than *E. coli* under the same starting conditions. The higher band intensities of target proteins in samples of *V. natriegens* suggest a higher proportion of target protein per µg loaded protein in comparison to *E. coli*.

A different *ccm* operon structure enables *V. natriegens* to produce holo-c-type cytochromes under aerobic conditions

Both *V. natriegens* and *E. coli* possess chromosomal copies of the *ccm* genes. The *E. coli* Cytc maturation has been intensely studied, although exact functions of some of the eight proteins are still not entirely clear[3–5]. While CcmA and CcmB are predicted to be transporter proteins it is unclear what substrate they transport. CcmC, CcmE, as well as CcmF deliver heme to the apo-Cytc while CcmD seems to stabilize CcmE in the membrane.

Electrons for the thioether bond formation between the cysteines and heme are delivered from a cytoplasmic thioreductase to DsbD, which transfers the electrons to CcmG and CcmH (Fig. 1). In *V. natriegens,* CcmH is a much smaller protein while the CcmI encoding gene presents an additional gene in the *ccm* operon. The CcmH from *E. coli* seems to be a fusion protein consisting of two domains. The N-terminal domain is homologous to Ccl2/CycL, a heme biogenesis protein present in *Rhodobacter capsulatus* and *Bradyrhizobium japonicum*[39]. The C-terminal domain is homologous to CcmI/CycH from other microorganisms, such as *R. capsulatus*[39] and *V. cholerae*[40]. Interestingly, the C-terminal CcmH domain of *E. coli* lacks the N-terminal portion of CcmI/CycH which is required for the biogenesis of c_1 cytochromes[39] since *E. coli* does not possess a cytochrome bc_1 complex. The C-terminal domain seems also not essential for Cytc maturation in *E. coli*[41]. The chromosomal *ccm* operon structures of *V. natriegens* ATCC 14048 (original strain from which V_{max} X2 was derived) and *E. coli* BL21(DE3) (T7 Express is a BL21 derivative) are depicted in Fig. 4.

In *E. coli*, the *ccm* genes are part of the *aeg46.5* operon together with the *nap* genes, encoding a periplasmic nitrate reductase[42]. Expression of all genes in this operon is only activated under anaerobic conditions[6]. A fumarate nitrate regulator (FNR)[43] binding site was predicted in the promoter region upstream of *napF* (Supplementary Note 3). FNR is a global positive regulator for the expression of genes required for anaerobic metabolism in *E. coli*[43,44]. The protein contains an oxygen-sensitive $[4Fe\text{-}4S]^{2+}$ cluster in its functional state under anaerobic conditions, increasing dimerization and site-specific DNA-binding. Under oxygen-limited conditions and in the presence of nitrate as a terminal electron acceptor, transcription of the *aeg46.5* operon in *E. coli* is activated. In addition to the *napABCDFGH* genes, the *ccmABCDEFGH* genes are also encoded on this operon since the *E. coli* nitrate reductase complex contains heme c which must be synthesized accordingly[6]. Contrarily, the *ccm* genes in *V. natriegens* form a separate operon on chromosome 1, while the *nap* genes are distributed across chromosome 2. Chromosomal promoter prediction revealed a potential promoter region upstream of *ccmA*. A RpoD16 binding site was predicted in this region (Supplementary Note 3). The *rpoD* gene product is the σ^{70} factor which is responsible for the transcription of genes during exponential aerobic growth[45].

Conclusion

Our study demonstrates that *V. natriegens* is a promising host for the production of c-type cytochromes for several reasons: (1) it can produce holo-c-type cytochromes without co-expressing additional genes from a second plasmid, (2) the supplementation of heme or its pre-cursors is not necessary to obtain holo-c-type cytochromes, (3) the proportion of target protein per µg loaded protein in *V. natriegens* was higher than in *E. coli*, (4) it exhibits faster growth and higher biomass production than *E. coli*. Our results demonstrate that expression vectors and strategies as well as codon-optimized gene sequences for *E. coli* can be easily transferred to *V. natriegens*. We were able to show that a switch can be beneficial for the heterologous production of proteins with complex co-factors, such as heme c, that *E. coli* struggles to integrate and especially for the production of membrane-anchored proteins. *V. natriegens* was capable of producing an electron transfer chain from an extremely acidophilic bacterium spanning both membranes and the periplasm. In future studies we hope to demonstrate the in vivo functionality of this electron transfer chain in *V. natriegens*.

Methods

Strains and plasmids

E. coli NEB5α (New England BioLabs) was used for plasmid propagation and purification. *E. coli* T7 Express (New England BioLabs) and *V. natriegens* V_{max} X2 (TelesisBio) were used for heterologous gene expression. Coding sequences of the four redox proteins CycA2, Cyc1A, Rus, and Cyc2A were obtained from GenBank (accession number QKQP01000005.1; locus-tags DN052_09955, DN052_11970, DN052_11940, and DN052_11975). All gene sequences were codon optimized for *E. coli* K-12 with JCat[46] (http://www.jcat.de/Start.jsp). Signal peptides were predicted with SignalP6.0[47] (https://services.healthtech.dtu.dk/services/SignalP-6.0/). Protein properties for apo- and holo-proteins alike were predicted with ProtParam[48] (https://web.expasy.org/protparam/). Original and

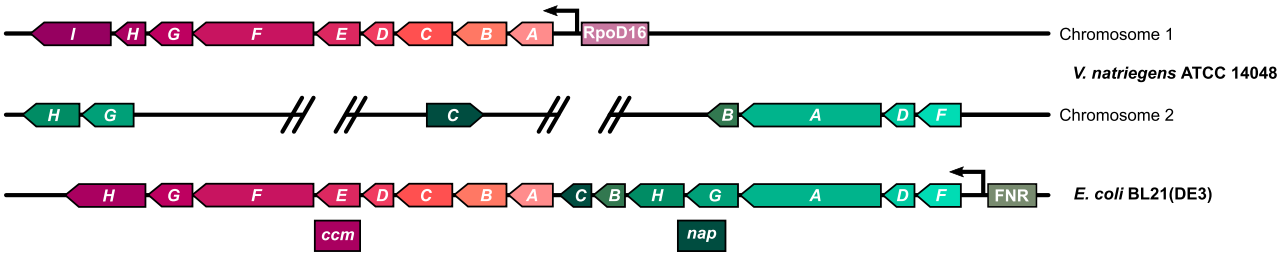

Figure 4. Comparison of the chromosomal *ccm* operon organization in *V. natriegens* and *E. coli*. The *ccm* genes (cytochrome c maturation; red) in *V. natriegens* form a separate operon on chromosome 1, while the *nap* genes (green), encoding a periplasmic nitrate reductase[42], are distributed across chromosome 2. Chromosomal promoter prediction revealed a potential promoter region upstream of *ccmA*. A RpoD16 binding site was predicted in this region, suggesting that the *ccm* genes are expressed during exponential aerobic growth. In *E. coli* the *ccm* genes are part of the *aeg46.5* operon together with the *nap* genes. Expression of all genes in this operon is only activated under anaerobic conditions[6]. A fumarate nitrate regulator (FNR)[43] binding site was predicted in the promoter region upstream of *napF*.

optimized gene and protein sequences are listed in Supplementary Note 1. Prediction results are available in Supplementary Note 2. Optimized gene sequences were synthesized, cloned into a pUC57 plasmid, and sequenced by GeneCust (Boynes, France). Vector maps are available in Supplementary Figs. 4–7. Plasmid sequences are available in Supplementary Data 1. The pEC86 vector encoding the *ccmABCDEFGH* genes from *E. coli* was obtained from the Culture Collection of Switzerland (CCOS891). The pET16bP vector was obtained from U. Wehemeyer (unpublished). The plasmid sequence is available in Supplementary Data 1.

The pET16bP_cycA_cyc1_rus_cyc2 expression vector was obtained by cloning restriction digestion fragments of all genes into the *Nco*I/*Not*I restriction site of the pET16bP vector. The ribosome binding site (RBS) and linker of the pET16b vector was cloned upstream of each gene. Successful cloning of all genes was confirmed by sequencing (Eurofins). A vector map is available in Supplementary Fig. 8. The plasmid sequence is available in Supplementary Data 1. The pEC86 and pET16bP_cycA_cyc1_rus_cyc2 vectors were successively transformed into *E. coli* T7 Express and *V. natriegens* V_{max} X2 via heat shock transformation, according to the manufacturer's instructions. Chemically competent cells containing the pEC86 vector were prepared as described below. All strains, primers, and plasmids used in this study are listed in Supplementary Table 1. Antibiotic concentrations used for selection and media recipes are listed in Supplementary Tables 2 and 3.

Preparation of chemically competent cells

After heat shock transformation of the pEC86 vector, *E. coli* T7 Express and *V. natriegens* V_{max} X2 were cultivated on Luria–Bertani (LB) plates (+ v2 salts) with appropriate antibiotics at 37 °C overnight. Pre-cultures (20 mL, LB [+ v2 salts]) containing appropriate antibiotics were inoculated from a single colony and incubated at 37 °C (30 °C for V_{max} X2) and 120 rpm overnight. 50 mL of LB (+ v2 salts) medium in a 250 mL baffled flask with appropriate antibiotics was inoculated to an $OD_{600} \approx 0.05$ and incubated at 37 °C (30 °C for V_{max} X2) and 120 rpm. Cells were harvested at 4 °C, 5000 *xg* for 10 min when the OD_{600} reached 0.5. Cells were subsequently handled on ice and all buffers and reaction tubes were pre-cooled on ice. Cells from a 50 mL culture were carefully resuspended in 16 mL CCMB80 buffer (10 mM potassium acetate, 80 mM $CaCl_2 \cdot 2H_2O$, 20 mM $MnCl_2 \cdot 2H_2O$, 10 mM $MgCl_2 \cdot 6H_2O$, 25% [v/v] glycerol, pH 6.4) and left on ice for 20 min. Cells were centrifuged (4 °C, 5000 x*g*, 10 min) and gently resuspended in 16 mL (or 650 µL for V_{max} X2) CCMB80 buffer. Chemically competent cells were either used directly for heat shock transformation according to the manufacturer's instructions or frozen in liquid N_2 and stored at − 80 °C.

Heterologous protein production

Cells from a cryo-stock were streaked on a LB (+ v2 salts) agar plate containing appropriate antibiotics. Plates were incubated at 37 °C (30 °C for V_{max} X2) overnight or at room temperature over two days. Pre-cultures were inoculated from a single colony and incubated at 37 °C (30 °C for V_{max}) and 120 rpm overnight. Enhanced 2xYT medium (e2xYT), supplemented with v2 salts when necessary, was used for pre-cultures. For V_{max} X2, e2xYT based ZYM-5052 + v2 salts autoinduction medium according to Studier[49] was used for expression, while *E. coli* T7 Express was cultivated in e2xYT medium. Expressions were carried out in 250 mL baffled flasks containing 50 mL medium and appropriate antibiotics. Main cultures were inoculated to an OD_{600} of 0.05 and incubated at 30 °C and 120 rpm. When the OD_{600} reached 0.6, 10 µM IPTG was added to *E. coli* cultures and all cultures were transferred to 25 °C and shaken at 120 rpm overnight. Since highly concentrated complex media were used for expression, heme or its pre-cursors were not supplied to the medium. Growth curves are available in Supplementary Fig. 3.

Cell fractionation

Fractionation of periplasmic, cytoplasmic, and membrane proteins was performed following the protocol of Petiti et al.[50]. All steps were performed at 4 °C or on ice, all buffers were pre-cooled on ice. Cells from a 50 mL culture were harvested at 5000 x*g* for 5 min. The cell wet weight is available in Supplementary Table 4. Pellets were carefully resuspended in 500 µL TES buffer (200 mM Tris–HCl pH 8.0, 0.5 mM EDTA, 0.5 M sucrose). 120 U lysozyme (in TES buffer) and 1.8 mL TES diluted 1:2 in water were added. Cells were shaken horizontally on ice for 30 min and centrifuged at 5000 x*g* for 5 min (8 min for V_{max} X2). The supernatant was kept as the periplasmic fraction (P). Spheroplasts were resuspended in 10 mL TES diluted 1:2 in water. One Pierce Protease Inhibitor Tablet (Thermo Scientific), 2 mM $MgCl_2 \cdot 6H_2O$, and 40 U DNaseI were added. Spheroplasts were disrupted by sonication at 70% intensity twice for 30 s and centrifuged at 2000 x*g* for 5 min (8 min for V_{max}). The supernatant was labelled as the cytoplasmic and membrane fraction (C + M) and centrifuged at 40,000 x*g* for 2 h to pellet membranes. The membranes (M) were resuspended in 2.5 mL TES diluted 1:2 in water overnight and the supernatant was kept as the cytoplasmic fraction (C). The total protein concentration of each fraction was determined in a 96-well plate with the Pierce BCA protein assay kit (Thermo Scientific) using triplicates according to the manufacturer's instructions. Calibration was performed according to the manufacturer's instructions with bovine serum albumin (BSA) in 1:2 diluted TES buffer in a 96-well plate using triplicates. TES buffer diluted 1:2 with water was used as blank for all measurements. The BCA assay results available in Supplementary Table 5. Samples for SDS-PAGE analysis were prepared for each fraction by mixing 200 µL sample (diluted with TES when necessary) with 100 µL 6× Laemmli buffer (375 mM Tris–HCl [pH 6.4], 9% [w/v] SDS, 0.03% [w/v] bromophenol blue, 50% [v/v] glycerol) and denatured at 95 °C for 5 min. The periplasmic fractions were concentrated 5× in a VivaSpin 500 centricon (molecular weight cut-off 10,000 Da) and prepared for SDS-PAGE analysis accordingly.

SDS-PAGE and Western blotting

SDS-PAGE was performed with Novex WedgeWell 10–20% Tris–Glycine gels (Thermo Scientific). Frozen denatured samples were thawed at 40 °C and centrifuged for 2 min at full speed. 150 µg total protein was loaded

onto the gel. For concentrated periplasmic fractions 300 µg total protein was used. PageRuler Plus Prestained Protein Ladder (Thermo Scientific) was used as size marker. When necessary, 0.33 µg of purified rusticyanin from *At. ferrooxidans*, kindly provided by Marianne Ilbert (Bioenergetic and Protein Engineering Laboratory, BIP, Institute of Microbiology of the Mediterranean, IMM), was used as positive control for immunodetection. Separation was performed in a Tris–glycine running buffer (25 mM Tris, 192 mM glycine, 0.1% [w/v] SDS, pH 8.3) at 125 V. Western blotting of gels was performed with the Mini Gel Tank and Blot Module Set (Thermo Scientific). Proteins were transferred to a PVDF membrane (pore size 0.2 µm) for 1 h at 20 V in a Tris–glycine transfer buffer (12 mM Tris–HCl [pH 8.3], 96 mM glycine).

TMBZ-staining of SDS-PAGE gels

TMBZ-staining was performed according to Thomas et al.[34]. This staining method relies on the peroxidase activity of heme. SDS-PAGE gels containing heme proteins are incubated in a TMBZ solution. Oxidation of TMBZ is catalysed by the peroxidase activity of the heme group upon addition of H_2O_2, leading to a blue precipitate. SDS-PAGE gels were incubated in seven parts 250 mM sodium acetate pH 5.0 and three parts 6.3 mM TMBZ in methanol for 2 h in the dark without shaking. 50–150 µL 30% hydrogen peroxide was added for colorimetric detection of covalently bound heme c. Gels were incubated in seven parts 250 mM sodium acetate pH 5.0 and three parts 2-propanol immediately after staining and kept in this solution in the dark without shaking overnight. Gels were visualized with a ChemiDoc XRS + gel imaging system (Bio-Rad) running ImageLab software (Bio-Rad). Unprocessed gel images are available in Supplementary Figs. 10 and 12.

Immunodetection

Membranes were blocked by incubation in TBS-T (19.3 mM Tris, 150 mM NaCl, 0.1% [v/v] Tween 20, pH 7.6) with 5% (w/v) non-fat dried milk powder for 60 min under gentle shaking. The primary rabbit anti-Rus antibody was diluted 1:1000 in TBS-T containing 5% (w/v) non-fat dried milk powder. Rabbit anti-Rus antibodies were kindly provided by Marianne Ilbert (Bioenergetic and Protein Engineering Laboratory, BIP, Institute of Microbiology of the Mediterranean, IMM). Membranes were incubated with primary antibodies for 1 h under gentle shaking. Afterwards, membranes were washed for a total of 30 min with TBS-T and incubated with Pierce goat anti-rabbit IgG-HRP secondary antibodies (Thermo Scientific) for 1 h under gentle shaking. Secondary antibodies were diluted 1:5000 with TBS-T containing 5% (w/v) non-fat dried milk powder. After a second washing step with TBS-T, 1-Step Ultra TMB-Blotting Solution (Thermo Scientific) was added for colorimetric detection. Membranes were visualized with a ChemiDoc XRS + gel imaging system (Bio-Rad) running ImageLab software (Bio-Rad). Unprocessed images are available in Supplementary Figs. 9 and 11.

UV/Vis spectroscopy

UV/Vis spectroscopy was performed with a Specord 50 Plus spectrometer (Analytik Jena) running WinAspect Plus (Analytik Jena). Absorbance was measured from 390 to 750 nm in increments of 0.5 nm. Measurements were carried out in TES buffer diluted 1:2 in water (as prepared). Samples were incubated for 30 min on ice with up to 10 mM $Na_2[IrCl_6]$ or a spatula tip of Na-dithionite for oxidation or reduction respectively. Buffer absorbance was used as a reference. All recorded UV/Vis spectra are available in Supplementary Figs. 13 and 14.

Prediction of chromosomal promoters

Bacterial promoters were predicted with BPROM[51] (http://www.softberry.com/berry.phtml?topic=bprom&group=programs&subgroup=gfindb) using only the operon sequence with its upstream region as input. Genomic sequences for *V. natriegens* ATCC 14048 (accession numbers NZ_CP016345 and NZ_CP016346) and *E. coli* BL21(DE3) (accession number NZ_CP053602) were retrieved from GenBank. Input sequences and results are listed in Supplementary Note 3.

Data availability

Accession numbers and locus-tags for existing gene and genome sequences retrieved from GenBank are listed in the appropriate Methods sections and in Supplementary Notes 1 and Note 3. The plasmid sequences and unprocessed gel images are available in Supplementary Data 1 and Supplementary Figs. 9–12 respectively. BCA assay results and UV/Vis spectra are available in Supplementary Table 5 and Supplementary Figs. 13 and 14. Sequencing results and raw data (BCA assay, UV/Vis spectra) that support the findings of this study are available from the corresponding author upon reasonable request. The authors declare that all other data supporting the findings of this study are available within the paper and its supplementary information files.

Received: 14 November 2023; Accepted: 8 February 2024
Published online: 13 March 2024

References

1. Liu, J. *et al.* Metalloproteins containing cytochrome, iron-sulfur, or copper redox centers. *Chem. Rev.* **114**, 4366–4469 (2014).
2. Londer, Y. Y. Expression of recombinant cytochromes c in *E. coli* in *heterologous gene expression in E. coli,* edited by T. C. Evans & M.-Q. Xu (Springer Science+Business Media LLC, 2011), 123–150.
3. Feissner, R. E. *et al.* Recombinant cytochromes c biogenesis systems I and II and analysis of haem delivery pathways in *Escherichia coli*. *Mol. Microbiol.* **60**, 563–577 (2006).
4. Thöny-Meyer, L., Fischer, F., Künzler, P., Ritz, D. & Hennecke, H. *Escherichia coli* genes required for cytochrome c maturation. *JB* **177**, 4321–4326 (1995).
5. Thöny-Meyer, L. Cytochrome c maturation: A complex pathway for a simple task?. *Biochem. Soc. Trans.* **30**, 633–638 (2002).

6. Grove, J. *et al. Escherichia coli* K-12 genes essential for the synthesis of c-type cytochromes and a third nitrate reductase located in the periplasm. *Mol. Microbiol.* **19**, 467–481 (1996).
7. Arslan, E., Schulz, H., Zufferey, R., Künzler, P. & Thöny-Meyer, L. Overproduction of the *Bradyrhizobium japonicum* c-type cytochrome subunits of the cbb_3 oxidase in *Escherichia coli*. *Biochem. Biophys. Res. Commun.* **251**, 744–747 (1998).
8. Rivera, M. & Walker, F. A. Biosynthetic preparation of isotopically labeled heme. *Anal. Biochem.* **230**, 295–302 (1995).
9. Fiege, K., Querebillo, C. J., Hildebrandt, P. & Frankenberg-Dinkel, N. Improved method for the incorporation of heme cofactors into recombinant proteins using *Escherichia coli* Nissle 1917. *Biochemistry* **57**, 2747–2755 (2018).
10. Varnado, C. L. & Goodwin, D. C. System for the expression of recombinant hemoproteins in *Escherichia coli*. *Protein Expression Purification* **35**, 76–83 (2004).
11. Eagon, R. G. *Pseudomonas natriegens*, a marine bacterium with a generation time of less than 10 minutes. *JB* **83**, 736–737 (1962).
12. Zhu, M., Mu, H., Jia, M., Deng, L. & Dai, X. Control of ribosome synthesis in bacteria: The important role of rRNA chain elongation rate. *Sci. China Life Sci.* **64**, 795–802 (2021).
13. Des Soye, B. J., Davidson, S. R., Weinstock, M. T., Gibson, D. G. & Jewett, M. C. Establishing a high-yielding cell-free protein synthesis platform derived from *Vibrio natriegens*. *ACS Synthetic Biol.* **7**, 2245–2255 (2018).
14. Hoffart, E. *et al.* High substrate uptake rates empower *Vibrio natriegens* as production host for industrial biotechnology. *Appl. Environ. Microbiol.* **83**, 01614-17 (2017).
15. Ellis, G. A. *et al.* Exploiting the feedstock flexibility of the emergent synthetic biology chassis *Vibrio natriegens* for engineered natural product production. *Mar. Drugs* **17**, 679 (2019).
16. Weinstock, M. T., Hesek, E. D., Wilson, C. M. & Gibson, D. G. *Vibrio natriegens* as a fast-growing host for molecular biology. *Nat. Methods* **13**, 849–851 (2016).
17. Eichmann, J., Oberpaul, M., Weidner, T., Gerlach, D. & Czermak, P. Selection of high producers from combinatorial libraries for the production of recombinant proteins in *Escherichia coli* and *Vibrio natriegens*. *Front. Bioeng. Biotechnol.* **7**, 254 (2019).
18. Tschirhart, T. *et al.* Synthetic biology tools for the fast-growing marine bacterium *Vibrio natriegens*. *ACS Synthetic Biol.* **8**, 2069–2079 (2019).
19. Lee, H. H. *et al. Vibrio natriegens*, a new genomic powerhouse. *bioRxiv,* 58487. https://doi.org/10.1101/058487 (2016).
20. Lee, H. H. *et al.* Functional genomics of the rapidly replicating bacterium *Vibrio natriegens* by CRISPRi. *Nat. Microbiol.* **4**, 1105–1113 (2019).
21. Dalia, T. N. *et al.* Multiplex genome editing by natural transformation (MuGENT) for synthetic biology in *Vibrio natriegens*. *ACS Synthetic Biol.* **6**, 1650–1655 (2017).
22. Stukenberg, D., Hoff, J., Faber, A. & Becker, A. NT-CRISPR, combining natural transformation and CRISPR-Cas9 counterselection for markerless and scarless genome editing in *Vibrio natriegens*. *Commun. Biol.* **5**, 265 (2022).
23. Schleicher, L. *et al. Vibrio natriegens* as host for expression of multisubunit membrane protein complexes. *Front. Microbiol.* **9**, 2537 (2018).
24. Becker, W., Wimberger, F. & Zangger, K. *Vibrio natriegens*: An alternative expression system for the high-yield production of isotopically labeled proteins. *Biochemistry* **58**, 2799–2803 (2019).
25. Xu, J. *et al. Vibrio natriegens* as a pET-compatible expression host complementary to *Escherichia coli*. *Front. Microbiol.* **12**, 627181 (2021).
26. Kormanová, Ľ *et al.* Comparison of simple expression procedures in novel expression host *Vibrio natriegens* and established *Escherichia coli* system. *J. Biotechnol.* **321**, 57–67 (2020).
27. Kucera, J. *et al.* A model of aerobic and anaerobic metabolism of hydrogen in the extremophile *Acidithiobacillus ferrooxidans*. *Front. Microbiol.* **11**, 610836 (2020).
28. Jiang, V., Khare, S. D. & Banta, S. Computational structure prediction provides a plausible mechanism for electron transfer by the outer membrane protein Cyc2 from *Acidithiobacillus ferrooxidans*. *Protein Sci.* **30**, 1640–1652 (2021).
29. Tsirigotaki, A., de Geyter, J., Šoštaric, N., Economou, A. & Karamanou, S. Protein export through the bacterial Sec pathway. *Nat. Rev. Microbiol.* **15**, 21–36 (2017).
30. Bengrine, A. *et al.* Sequence and expression of the rusticyanin structural gene from *Thiobacillus ferrooxidans* ATCC33020 strain. *Biochimica et Biophysica Acta (BBA) Gene Struct. Expression* **1443**, 99–112 (1998).
31. Cobley, J. G. & Haddock, B. A. The respiratory chain of *Thiobacillus ferrooxidans*: The reduction of cytochromes by Fe^{2+} and the preliminary characterization of rusticyanin a novel "blue" copper protein. *FEBS Lett.* **60**, 29–33 (1975).
32. Mansch, R. Acid-stable cytochromes in ferrous ion oxidizing cell-free preparations from *Thiobacillus ferrooxidans*. *FEMS Microbiol. Lett.* **92**, 83–87 (1992).
33. Castelle, C. *et al.* A new iron-oxidizing/O_2-reducing supercomplex spanning both inner and outer membranes, isolated from the extreme acidophile *Acidithiobacillus ferrooxidans*. *J. Biol. Chem.* **283**, 25803–25811 (2008).
34. Thomas, P. E., Ryan, D. & Levin, W. An improved staining procedure for the detection of the peroxidase activity of cytochrome P-450 on sodium dodecyl sulfate polyacrylamide gels. *Anal. Biochem.* **75**, 168–176 (1976).
35. Yamanaka, T. *The biochemistry of bacterial cytochromes. With 33 tables* (Springer; Japan Scientific Soc. Press, 1992).
36. Abramson, J. *et al.* The structure of the ubiquinol oxidase from *Escherichia coli* and its ubiquinone binding site. *Nat. Struct. Biol.* **7**, 910–917 (2000).
37. Fang, H., Lin, R. J. & Gennis, R. B. Location of heme axial ligands in the cytochrome d terminal oxidase complex of *Escherichia coli* determined by site-directed mutagenesis. *J. Biol. Chem.* **264**, 8026–8032 (1989).
38. Miller, M. J. & Gennis, R. B. The purification and characterization of the cytochrome d terminal oxidase complex of the *Escherichia coli* aerobic respiratory chain. *J. Biol. Chem.* **258**, 9159–9165 (1983).
39. Thöny-Meyer, L. Biogenesis of respiratory cytochromes in bacteria. *Microbiol. Mol. Biol. Rev. MMBR* **61**, 337–376 (1997).
40. Braun, M. & Thöny-Meyer, L. Cytochrome c maturation and the physiological role of c-type cytochromes in *Vibrio cholerae*. *JB* **187**, 5996–6004 (2005).
41. Grovc, J., Busby, S. & Cole, J. The role of the genes *nrfEFG* and *ccmFH* in cytochrome c biosynthesis in *Escherichia coli*. *Mol. General Genet. MGG* **252**, 332–341 (1996).
42. Potter, L. C. & Cole, J. A. Essential roles for the products of the *napABCD* genes, but not *napFGH*, in periplasmic nitrate reduction by *Escherichia coli* K-12. *Biochem. J.* **344**(Pt 1), 69–76 (1999).
43. Unden, G. & Trageser, M. Oxygen regulated gene expression in *Escherichia coli*: Control of anaerobic respiration by the FNR protein. *Antonie van Leeuwenhoek* **59**, 65–76 (1991).
44. Kiley, P. J. & Beinert, H. Oxygen sensing by the global regulator, FNR: The role of the iron-sulfur cluster. *FEMS Microbiol. Rev.* **22**, 341–352 (1998).
45. Jishage, M., Iwata, A., Ueda, S. & Ishihama, A. Regulation of RNA polymerase sigma subunit synthesis in *Escherichia coli*: Intracellular levels of four species of sigma subunit under various growth conditions. *JB* **178**, 5447–5451 (1996).
46. Grote, A. *et al.* JCat: A novel tool to adapt codon usage of a target gene to its potential expression host. *Nucleic Acids Res.* **33**, W526–W531 (2005).
47. Teufel, F. *et al.* SignalP 6.0 predicts all five types of signal peptides using protein language models. *Nat. Biotechnol.* **40**, 1023–1025 (2022).
48. Gasteiger, E. *et al.* Protein identification and analysis tools on the ExPASy server. in *The Proteomics Protocols Handbook* (Humana Press, 2005), 571–607.

49. Studier, F. W. Protein production by auto-induction in high density shaking cultures. *Protein Expression Purification* **41**, 207–234 (2005).
50. Petiti, M., Houot, L. & Duché, D. Cell fractionation. in *Methods in molecular biology (Clifton, N.J.)* **1615,** 59–64 (2017).
51. Solovyev, V. & Salamov, A. Automatic annotation of microbial genomes and metagenomic sequences. in *Metagenomics and its Applications in Agriculture, Biomedicine and Environmental Studies* (2011), 61–78.

Acknowledgements

The authors thank Violaine Bonnefoy and Marianne Ilbert (Bioenergetic and Protein Engineering Laboratory, BIP, Institute of Microbiology of the Mediterranean, IMM) for their generous gift of anti-Rus antibodies, as well as purified rusticyanin. H. F. acknowledges support from the Deutsche Bundesstiftung Umwelt (DBU, German Federal Environmental Foundation, Grant number 20021/731 to H. F.). S. R. U. acknowledges support from the Deutsche Forschungsgemeinschaft (DFG, German Research Foundation, Grant number UL5081-1 to S. R. U.). The funders had no role in study design, data collection and analysis, or decision to publish.

Author contributions

H.F. conceptualized the study, carried out the experiments, and prepared the manuscript. S.R.U. and S.H. supervised the study. All authors read and approved the final manuscript.

Funding

Open Access funding enabled and organized by Projekt DEAL.

Competing interests

The authors declare no competing interests.

Additional information

Supplementary Information The online version contains supplementary material available at https://doi.org/10.1038/s41598-024-54097-7.

Correspondence and requests for materials should be addressed to H.F. or S.H.

Reprints and permissions information is available at www.nature.com/reprints.

Publisher's note Springer Nature remains neutral with regard to jurisdictional claims in published maps and institutional affiliations.